Non-Linear Autoregressive Dissolved Oxygen Prediction Model for Paddy Irrigation Channel

Syafira Mohd Aisha [1], Norashikin M. Thamrin [1], Muhammad Fariq Ghazali [2], Nik Nor Liyana Nik Ibrahim [3], Megat Syahirul Amin Megat Ali [4]

[1]*School of Electrical Engineering, College of Engineering, Universiti Teknologi MARA, Shah Alam, Malaysia*
[2]*QES (Asia-Pacific) Sdn. Bhd., Shah Alam, Malaysia*
[3]*Department of Chemical and Environmental Engineering, Universiti Putra Malaysia, Serdang, Malaysia*
[4]*Microwave Research Institute, Universiti Teknologi MARA, Shah Alam, Malaysia*

Abstract **– This study has proposed a non-linear autoregressive model to predict one-day ahead dissolved oxygen in paddy field irrigation channel. A 32-day data is obtained from Kampung Padang To' La in Pasir Mas, Kelantan using off-the shelf water quality parameter sensors. Analysis has revealed no correlation between dissolved oxygen with pH and electrical conductivity. A non-linear autoregressive model is then developed using the dissolved oxygen measurements and artificial neural network. A prediction model developed using Levenberg-Marquardt algorithm yielded the best results with overall regression of 0.9253. The model has also passed all correlation tests and can therefore, be accepted.**

Keywords **– Paddy, non-linear autoregressive, neural network, dissolved oxygen, Levenberg-Marquardt.**

1. Introduction

More than half of the global population consumes rice as a staple food [1]. The steady chain of rice supply is made possible through the irrigation channels that flood the paddy fields with water.

DOI: 10.18421/TEM112-43
https://doi.org/10.18421/TEM112-43

Corresponding author: Megat Syahirul Amin Megat Ali,
Microwave Research Institute, Universiti Teknologi MARA, Shah Alam, Malaysia
Email: megatsyahirul@uitm.edu.my

Received: 17 March 2022.
Revised: 08 May 2022.
Accepted: 13 May 2022.
Published: 27 May 2022.

Concerns have also risen on the existence of poultry farms and factories within the vicinity as they present a source of contamination that could affect the quality of rice paddy [2]. Therefore, monitoring systems are needed to assess the quality of water flowing into the fields. This is defined in terms of chemical, physical and biological characteristics of water based on the standards of its usage [3]. Thus far, dissolved oxygen (DO) is among the most vital parameters. The DO refers to the level of free, non-compound oxygen that is present in the water [4]. Water sources that are contaminated with manure and fertilizers increases unwanted nitrates. These increases growth of algae and microorganisms [5]. The increased algae population blocks light from reaching aquatic plants. This deprives photosynthesis and reduces the amount of oxygen in the water. The algae population also uses up oxygen in the water body which then suffocates other aquatic species [6].

Low levels of DO will adversely affect the quality of paddy as the oxygen-rich water is required to promote root growth. The root uses oxygen for aerobic respiration which is an essential process that releases the energy in a healthy plant [7]. Therefore, monitoring the DO level in the irrigation channels could provide warning on the looming contamination in the water body, so that actions can be taken before it reaches the paddy fields. Two other parameters that could be used to assess water quality are pH [8] and electrical conductivity (EC) [9]. However, the DO does not directly affect pH as there is no physical-chemical connection between the two parameters. The pH is associated with the presence of free carbon dioxide (CO_2), while DO only refers to the number of oxygen atoms dissolved in water that does not form other molecules [10]. A contaminated body of water will have increased CO_2 due to the large algae population. These result in an acidic environment which reduces the water pH [11]. Meanwhile, the EC estimates the amount of total dissolved ions in the water. Increased salinity reduces oxygen solubility, thereby decreasing the level of DO [12].

To effectively monitor water contamination in the paddy field irrigation channels, the use of predictive models is required. These can be realized using machine learning methods such as artificial neural network (ANN) [13]. The technique emulates the function of neurons in the brain and generalizes a solution based on the provided examples [14]. The model can take on different network structures. A static ANN may simulate non-linear functions and thus, can be used for modelling time-series information. However, they may not always be able to develop accurate non-linear model that can predict system dynamics [15]. To overcome this, non-linear autoregressive with exogenous input (NARX) model structure can be utilized. Its use in time-series models have been successful, owing to its ability to accurately learn the relationship between variables even with limited dataset [16]. The NARX has also been widely used for environmental studies. These range from droughts and flood prediction [17], monitoring river contamination [18], air pollution forecasting [19], and prediction of ground water level [20].

Based on the literature review, two main problems have been identified. Firstly, the existence of nearby poultry farming, and plantation presents a source of contamination for the irrigation channels that supply water to the paddy fields. Thus far, no literature has directly observed and applied the DO, pH, and EC for monitoring the fluctuation of water quality in the irrigation channels. Secondly, a predictive model that could solve the issues have yet to be developed. Furthermore, the model will also need to be optimized for the best performance. Hence, the study sets out to: 1) determine the correlation between the DO, pH, and EC from the water in irrigation channels, 2) to develop and optimize the prediction model using NARX-based ANN. The findings will be beneficial to the DO prediction model that can be used to monitor impending contamination in the water. These could then be utilized by the authorities to take countermeasures in ensuring that the growth of rice paddy is not affected.

2. Methods

2.1. Data Sampling and Correlation Analysis

The DO, pH and EC are collected from the irrigation channel at Kampung Padang To' La in Pasir Mas, Kelantan. The sampling is performed twice daily at 12.00 pm and 7.00 pm for 32 days. All readings were taken using commercially available devices. Figure 1. shows the site of data collection on Google Map.

Figure 1. Data collection at Kampung To' La, Pasir Mas, Kelantan

Correlation analysis is then conducted for preliminary investigation. The coefficient represents the strength of relationship between the parameters x and y. The correlation coefficient, r_{xy}, is shown by (1), where x_i and y_i are the measured variables. Meanwhile, $\overline{x}$ and $\overline{y}$ each represent the mean value for the respective water quality parameters [21].

$$r_{xy} = \frac{\sum(x_i - \overline{x})(y_i - \overline{y})}{\sqrt{\sum(x_i - \overline{x})^2 \sum(y_i - \overline{y})^2}} \quad (1)$$

Generally, the value of r will range from –1 to 1 in which both indicate perfect correlation. The negative sign indicates inversed relationship, while a positive sign shows proportional relationship between the variables x and y. For the pH and EC to be used as input to the model, the correlation of DO with both parameters need to be larger than 0.3. Any value lesser than 0.3 indicates that the variables are uncorrelated [22].

2.2. ANN and NARX

ANN is a machine learning technique that emulates the biological function of neurons in the brain. This black box method generalizes a solution to a problem from given examples. Generally, the ANN provides a non-linear mapping of input vector to the output space [23]. Subsequently, NARX is a widely used dynamic model structure that can capture the behavior of non-linear systems. Initially, the model is developed in an open-loop series-parallel structure. After the training is complete, the model is tested in a closed-loop parallel configuration. These are shown in Figure 2.

The input-output relationship for open-loop and closed-loop structures are each defined by (2) and (3), where $\hat{y}(t)$ is the predicted output at time t and $F(.)$ is the estimated model. The input elements are given by $x(t)$, $x(t-1)$, $x(t-2)$, …, $x(t-n_x)$, and the past desired output by $y(t-1)$, $y(t-2)$, …, $y(t-n_y)$. In the closed-loop structure, the lagged predicted output from model is given by $\hat{y}(t-1)$, $\hat{y}(t-2)$, …, $\hat{y}(t-n_y)$. The number of lags for input and output are each denoted by n_x and n_y [24].

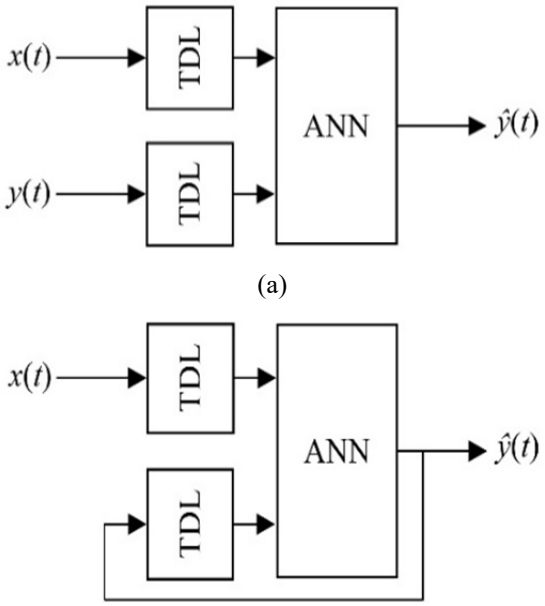

Figure 2. (a) Open-loop, and (b) closed-loop NARX structure with tapped delay lines (TDL)

$$\hat{y}(t) = F\big[y(t-1), y(t-2), \dots, y\big(t-n_y\big), x(t), x(t-1), x(t-2), \dots, x(t-n_x)\big] \quad (2)$$

$$\hat{y}(t) = F\big[\hat{y}(t-1), \hat{y}(t-2), \dots, \hat{y}\big(t-n_y\big), x(t), x(t-1), x(t-2), \dots, x(t-n_x)\big] \quad (3)$$

As a black box model, the mapping function $F(.)$ is initially unknown. The ANN is used to estimate the relationship between input and output variables. Generally, the network consists of an input layer, several hidden layers, and an output layer. It is worth noting that the number of hidden layers vary with application. In this study, however, two hidden layers should suffice for function approximation purposes. These are based on a recent study on modelling of WQI for a river that employed similar configuration with 20 nodes for the respective layers [25]. Figure 3. shows the structure of the ANN with two hidden layers. The output from the model is the measured DO. However, the selected input will depend on the correlation analysis between the DO, pH, and EC. As the study aims to perform a one-day ahead DO prediction, a TDL of two is used.

Initially, the input variables, x_i, are converted into a vector of variables, u_j, in the first hidden layer via activation function, Γ_1. This is shown by (4), where w_{ij} are the weights linking ith node in the input layer to jth node in the first hidden layer, and θ_j represents the biases in the first hidden layer. The number of input nodes is denoted by M.

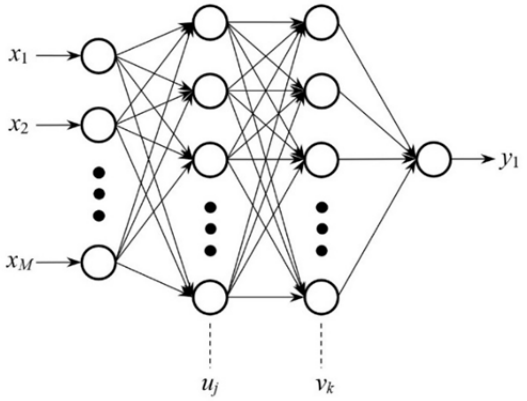

Figure 3. General structure of an ANN with two hidden layers

$$u_j = \Gamma_1\left(\sum_{i=1}^{M} w_{ij}x_i + \theta_j\right) \quad (4)$$

Using the same activation function, Γ_1, the vector of variables from the first hidden layer, u_j, is then converted into a vector of variables, v_k, in the second hidden layer. As shown in (5), w_{jk} are the weights linking jth node in the first hidden layer to kth node in the output layer. θ_k represents the biases in the second hidden layer and N is the number of nodes in the first hidden layer.

$$v_k = \Gamma_1\left(\sum_{j=1}^{N} w_{jk}u_j + \theta_k\right) \quad (5)$$

Subsequently, the vector of variables, v_k, from the second hidden layer is transformed to the output vector, y_l, through activation function, Γ_2. This is expressed by (6). w_{kl} are the weights linking kth node in the second hidden layer to lth node in the output layer. θ_l is the bias, and O is the number of nodes in the second hidden layer.

$$y_l = \Gamma_2\left(\sum_{k=1}^{O} w_{kl}v_k + \theta_l\right) \quad (6)$$

Γ_1 and Γ_2 are each hyperbolic tangent and pure linear activation functions. The dataset is divided for training, validation, and testing with 70:15:15 split ratio. During training, the network uses the error between the computed and desired output to perform back-propagation weight updates. Three learning algorithms are used to assess optimum performance; Levenberg-Marquardt (LM), Scaled Conjugate Gradient (SCG), and Resilient Propagation (RP) algorithms. Early stopping criterion is used to avoid the network from over-fitting. The validation dataset is implemented to assess generalization performance during training. If the validation error continues to increase, this indicates that the network has started to over-fit, and the training is halted [26]. To compare

network performance between the three learning algorithms, assessment is performed based on overall regression. As the initial weights and biases are influenced by the random number generator setting, this will result in a variation of performance. Hence, for every learning algorithm, 100,000 initial weights and biases configuration is tested.

After obtaining the best network performance out of the three learning algorithms, a more detailed analysis is performed using regression plots, error histogram, and time-series analysis. Generally, a model with good regression fit is associated with low error that is distributed close to 0. Autocorrelation (ACF) [27] and cross-correlation function (CCF) [28] tests are also conducted. The ACF test is performed to identify correlation between the residuals with itself at different time lags. Similarly, the CCF test assesses correlation but between the predicted output and the residuals. The error produced by the model should be random. Therefore, the residuals should not be correlated with itself or the predicted output. The correlation coefficients should fall within the 95% confidence interval, Δ [29]. This is defined by (7), where L is the sample size.

$$\Delta = \pm \frac{1.96}{\sqrt{L}} \tag{7}$$

3. Results and Discussion

3.1. Data acquisition and correlation analysis

The DO, pH and EC have been successfully measured for a duration of 32 days. Correlation analysis is performed on the DO-pH, DO-EC, and pH-EC parameters. The correlation coefficients obtained are shown in Table 1. Based on the results, the pH and EC are not correlated with the DO.

Table 1. Correlation coefficient among water quality parameters

Variable	DO	pH	EC
DO	1		
pH	0.02402	1	
EC	–0.02251	0.32154	1

While this is expected of the pH, similar observation contradicted the literature. However, it is worth noting that the analysis indicated negative association between the DO and the EC, albeit negligible. Such observation is valid as the irrigation channel is an open body of water, not a closed body like that of a lake. Therefore, changes to the EC do not directly affect the DO. Weak relationship, however, could be observed between the pH and EC. However, these could be ruled out as purely coincidental as the two parameters do not share physical-chemical relationship. The pH is related to movement of free hydrogen ions, while the EC is associated with movement of free electrons.

Since both the pH and the EC show no correlation with the DO, the DO will be used to predict its future output values. Therefore, the exogenous input component is removed from NARX, and the model is switched to a non-linear autoregressive model structure.

3.2. Non-linear Autoregressive DO Prediction Model

A total of 100,000 initial weights and biases are tested for LM, SCG and RP algorithms. The best overall regression for each algorithm is shown in Table 2. Through exhaustive testing, the best performance of 0.9253 was attained with LM algorithm. These agree with other studies that conduct similar comparison but for different machine learning application [30].

Table 2. The best performance for LM, SCG and RP algorithms

Learning algorithm	LM	SCG	RP
Best overall regression	0.9253	0.8492	0.8739

Subsequently, only results pertaining to the best model attained with LM algorithm are discussed. The regression plots for network training, validation, and testing are each shown in Figure 4. Satisfactory results have been obtained with values of 0.9731, 0.8225, and 0.7232, respectively. Training regression attained the highest regression as the model is exposed to larger amount of data. Meanwhile, the validation and testing datasets are unseen samples that are not considered during network training. These impact its ability to generalize a solution which led to lower regression values for both validation and testing.

The time-series response and error plots are shown in Figure 5. Based on these observations, it can be concluded that the excellent regression during training is complemented by low error. Conversely, the lower regression for validation and testing are reflected by the higher error. These are complemented by the histogram in Figure 6. indicating good results as majority of the errors are distributed close to 0. However, larger errors have also been observed. While errors close to 0 are contributed by the network training, the larger ones are from the validation and testing.

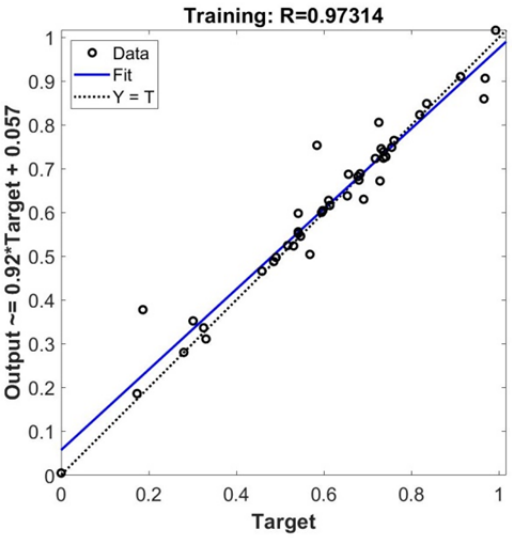

(a)

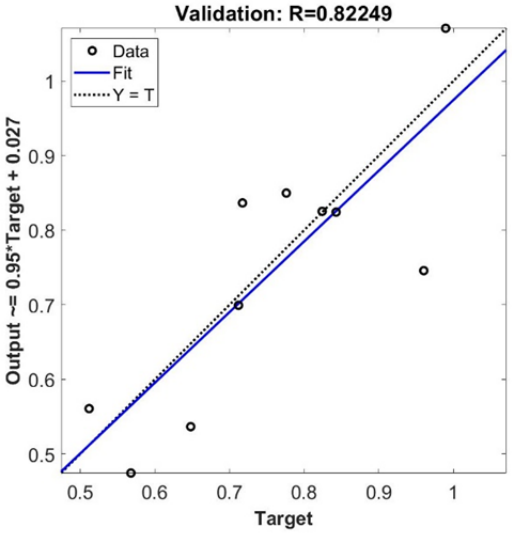

(b)

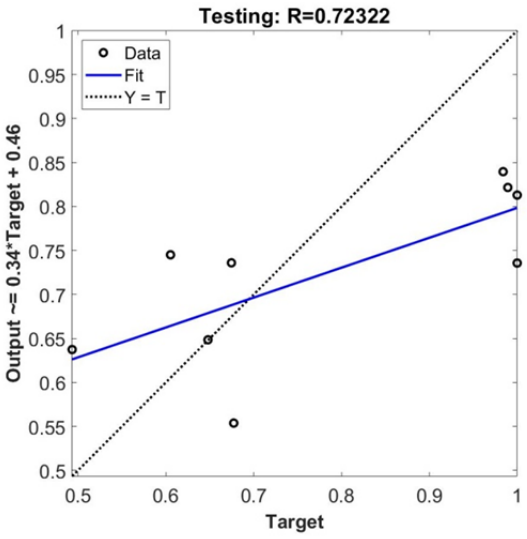

(c)

Figure 4. Regression plots for (a) training, (b) validation, and (c) testing

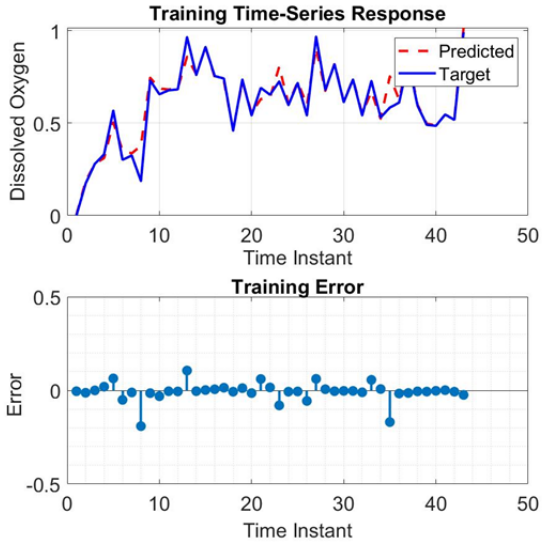

(a)

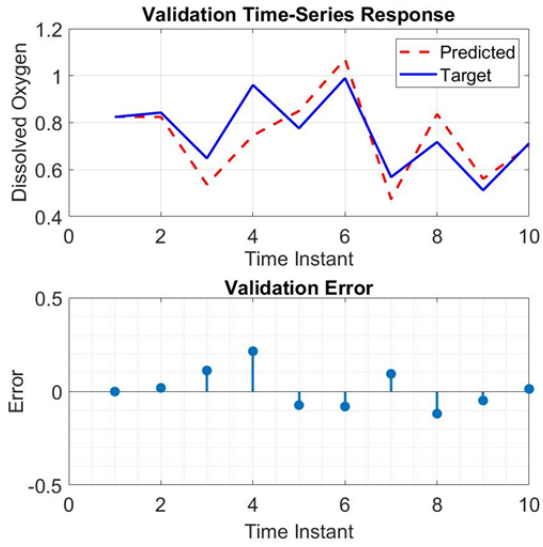

(b)

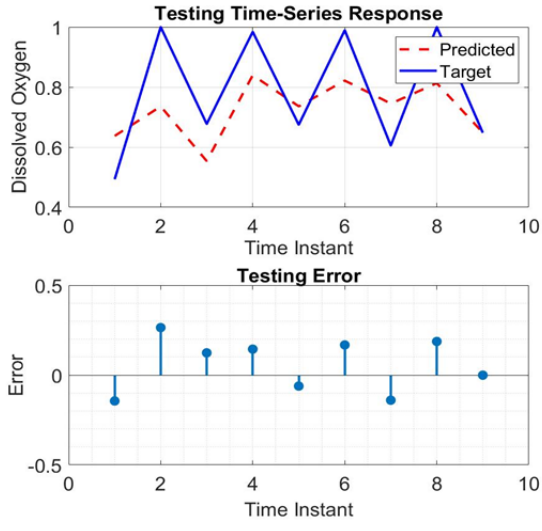

(c)

Figure 5. Time-series response and error for (a) training, (b) validation, and (c) testing

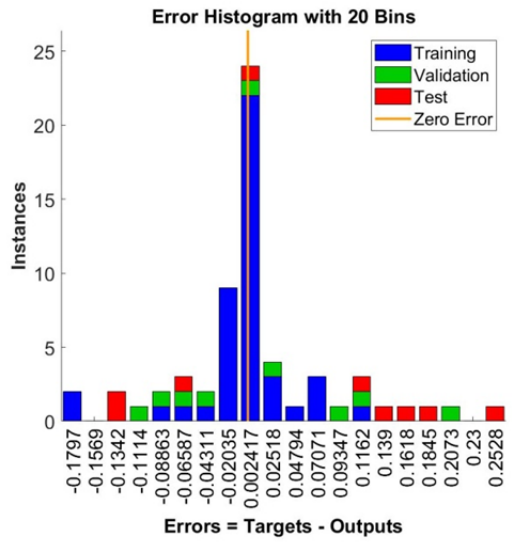

Figure 6. Error histogram

Figure 7. and Figure 8. each show the ACF and CCF tests for model training.

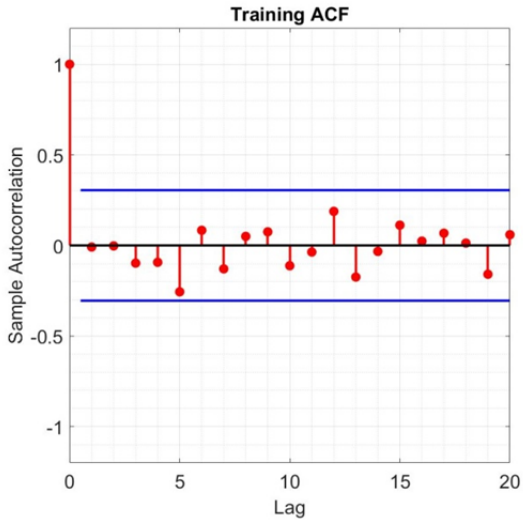

Figure 7. ACF test for network training

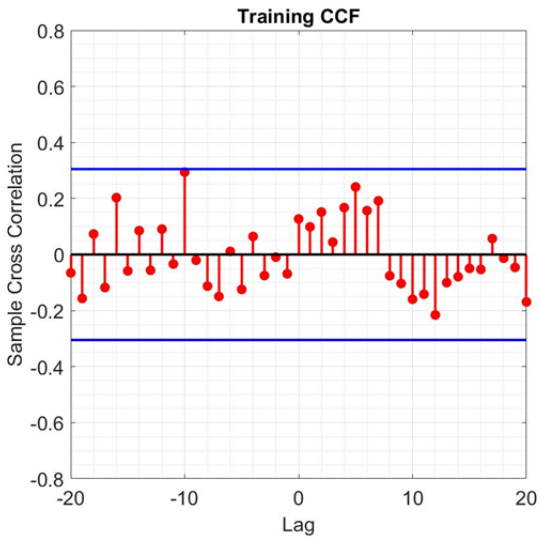

Figure 8. CCF test for network training

For the ACF test, the coefficients for all lags show no correlation except for lag 0. At lag 0, the residuals are perfectly correlated with itself, thereby yielding the coefficient of 1. For all other lags, the coefficients are well within the defined 95% confidence interval. The CCF test has further revealed that the residuals and the predicted outputs are also not correlated for all lags. Hence, the residuals produced by the model during training are random.

Meanwhile, the ACF and CCF tests for network validation are each shown in Figure 9. and Figure 10. Similar with the ACF test for network training, the coefficients indicate no correlation except lag 0. At lag 0, the residuals are perfectly correlated with itself. For all other lags, the coefficients fall within the 95% confidence interval. Based on the observed CCF test, the residuals and the predicted output indicate no correlation for all lags, indicating that the residuals for network validation are also random.

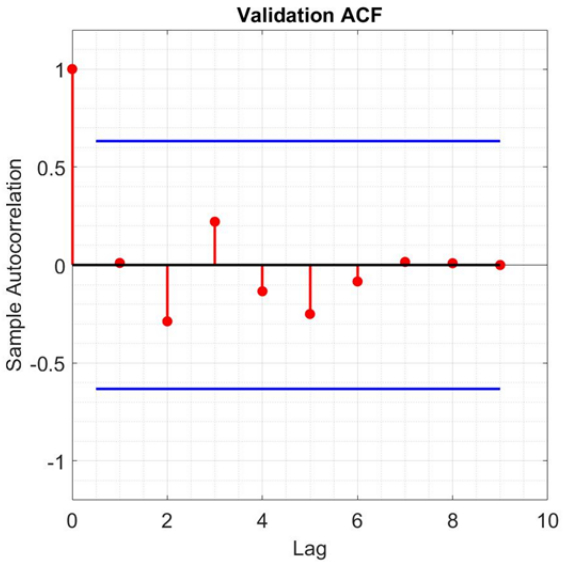

Figure 9. ACF test for network validation

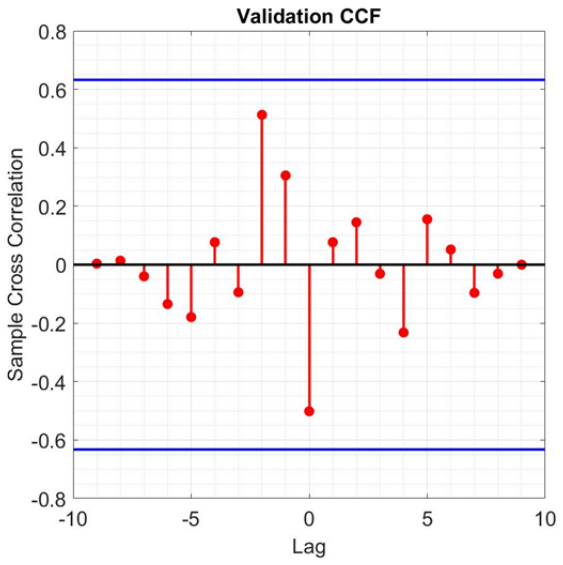

Figure 10. CCF test for network validation

Figure 11. and Figure 12. show the ACF and CCF tests for network testing, respectively. For ACF test, the coefficients revealed no correlation at all lags expect lag 0. Similar explanation applies where the residuals are perfectly correlated with itself, yielding coefficient of 1. For all other lags, the coefficients are within the 95% confidence interval. The CCF test further revealed that the residuals are not correlated with the predicted outputs for network testing. Hence, the residuals are also random, and the model has passed the correlation function test.

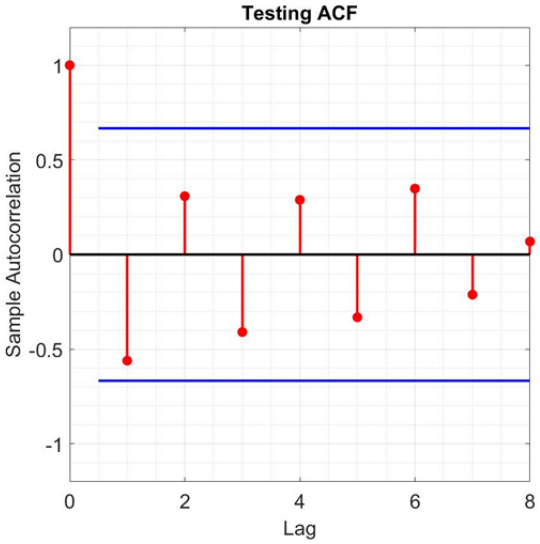

Figure 11. ACF test for network testing

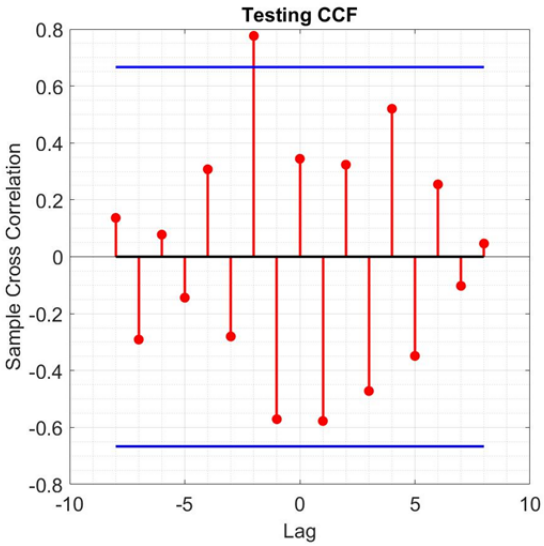

Figure 12. CCF test for network testing

4. Conclusion

Generally, the study has proposed to solve two major objectives. First, to determine the correlation between the DO, pH, and EC from the water in irrigation channels, and second, to develop and optimize the prediction model using NARX-based ANN. The DO, pH and EC measurements have been successfully collected at an irrigation channel in Kampung To' La, Pasir Mas, Kelantan. The relationship between the EC and DO is negligible as sampling is performed in an open body of water. Therefore, changes to the EC cannot be observed directly on the DO. As both pH and EC show no correlation with the DO, the input component to the model is removed. The structure is then reduced to that of a non-linear autoregressive model. Hence, the DO is used to predict its own future values. Subsequently, by performing exhaustive tests on different initial weights and biases on the learning algorithms, the study has revealed that the LM algorithm provides the best performance. Further analysis has revealed satisfactory regression and error for network training, validation, and testing. The model has also passed both the ACF and CCF tests, indicating the residuals generated are random.

However, the developed model is not without shortcomings. As observed from the validation and testing results, the model has the potential to be improved. Frequency of sampling and the period of data collection should be increased. These would allow the model to be trained using greater variation of data that are also influenced by weather factors. Furthermore, an extensive range of data will also allow prediction of the DO by more than one day. Hence, a more reliable and accurate prediction of future DO fluctuations would be desirable. Generally, the current model has been successfully developed. In its current state, the model can already perform a one-day ahead prediction. Therefore, it can be integrated into a system that can monitor contamination levels in the irrigation channel by employing the commercially available DO sensor. Should the predicted contamination exceed a certain limit, authorities can take countermeasures in ensuring that growth and quality of rice paddy are not affected.

Acknowledgements

The study is supported by Universiti Teknologi MARA through the LESTARI SDG-T grant (600-RMC/LESTARI SDG-T 5/3 (131/2019)).

References

[1]. Fukagawa, N. K., & Ziska, L. H. (2019). Rice: Importance for global nutrition. *Journal of nutritional science and vitaminology*, *65*(Supplement), S2-S3.

[2]. Cui, N., Cai, M., Zhang, X., Abdelhafez, A. A., Zhou, L., Sun, H., ... & Zhou, S. (2020). Runoff loss of nitrogen and phosphorus from a rice paddy field in the east of China: Effects of long-term chemical N fertilizer and organic manure applications. *Global Ecology and Conservation*, *22*, e01011.

[3]. Camara, M., Jamil, N. R., & Abdullah, A. F. B. (2019). Impact of land uses on water quality in Malaysia: a review. *Ecological Processes*, *8*(1), 1-10.

[4]. Salih, S. Q., Alakili, I., Beyaztas, U., Shahid, S., & Yaseen, Z. M. (2021). Prediction of dissolved oxygen, biochemical oxygen demand, and chemical oxygen demand using hydrometeorological variables: case study of Selangor River, Malaysia. *Environment, Development and Sustainability*, *23*(5), 8027-8046.

[5]. Ohadi, S., Laguerre, G., Madsen, J., & Al-Khatib, K. (2022). Toward understanding the impact of nuisance algae bloom on the reduction of rice seedling emergence and establishment. *Weed Science*, *70*(1), 95-102.

[6]. Wang, Q., Li, X., Yan, T., Song, J., Yu, R., & Zhou, M. (2021). Laboratory simulation of dissolved oxygen reduction and ammonia nitrogen generation in the decay stage of harmful algae bloom. *Journal of Oceanology and Limnology*, *39*(2), 500-507.

[7]. de Sousa Lopes, L., de Carvalho, H. H., de Souza Miranda, R., Gallao, M. I., & Gomes-Filho, E. (2020). The influence of dissolved oxygen around rice roots on salt tolerance during pre-tillering and tillering phases. *Environmental and Experimental Botany*, *178*, 104169.

[8]. Saalidong, B. M., Aram, S. A., Otu, S., & Lartey, P. O. (2022). Examining the dynamics of the relationship between water pH and other water quality parameters in ground and surface water systems. *PloS one*, *17*(1), e0262117.

[9]. Lintern, A., Webb, J. A., Ryu, D., Liu, S., Waters, D., Leahy, P., ... & Western, A. W. (2018). What are the key catchment characteristics affecting spatial differences in riverine water quality?. *Water Resources Research*, *54*(10), 7252-7272.

[10]. Usui, Y., & Kasubuchi, T. (2011). Effects of herbicide application on carbon dioxide, dissolved oxygen, pH, and RpH in paddy-field ponded water. *Soil Science and Plant Nutrition*, *57*(1), 1-6.

[11]. Raven, J. A., Gobler, C. J., & Hansen, P. J. (2020). Dynamic CO2 and pH levels in coastal, estuarine, and inland waters: Theoretical and observed effects on harmful algal blooms. *Harmful Algae*, *91*, 101594.

[12]. Ren, A. S., Chai, F., Xue, H., Anderson, D. M., & Chavez, F. P. (2018). A sixteen-year decline in dissolved oxygen in the central California Current. *Scientific reports*, *8*(1), 1-9.

[13]. Wagh, V., Panaskar, D., Muley, A., Mukate, S., & Gaikwad, S. (2018). Neural network modelling for nitrate concentration in groundwater of Kadava River basin, Nashik, Maharashtra, India. *Groundwater for Sustainable Development*, *7*, 436-445.

[14]. Silva, I. N., Spatti, D. H., Flauzino, R. A., Liboni, L. H. B., & Alves, S. R. (2017). Artificial neural networks: a practical course. *Switzerland: Springer International Publishing*.

[15]. Shoaib, M., Shamseldin, A. Y., Melville, B. W., & Khan, M. M. (2016). A comparison between wavelet based static and dynamic neural network approaches for runoff prediction. *Journal of Hydrology*, *535*, 211-225.

[16]. Gu, Y., & Wei, H. L. (2018). A robust model structure selection method for small sample size and multiple datasets problems. *Information Sciences*, *451*, 195-209.

[17]. Wang, J., & Chen, Y. (2022). Using NARX neural network to forecast droughts and floods over Yangtze River Basin. *Natural Hazards*, *110*(1), 225-246.

[18]. Di Nunno, F., Race, M., & Granata, F. (2022). A nonlinear autoregressive exogenous (NARX) model to predict nitrate concentration in rivers. *Environmental Science and Pollution Research*, 1-20.

[19]. Buevich, A., Sergeev, A., Shichkin, A., & Baglaeva, E. (2021). A two-step combined algorithm based on NARX neural network and the subsequent prediction of the residues improves prediction accuracy of the greenhouse gases concentrations. *Neural Computing and Applications*, *33*(5), 1547-1557.

[20]. Di Nunno, F., & Granata, F. (2020). Groundwater level prediction in Apulia region (Southern Italy) using NARX neural network. *Environmental Research*, *190*, 110062.

[21]. Gogtay, N. J., & Thatte, U. M. (2017). Principles of correlation analysis. *Journal of the Association of Physicians of India*, *65*(3), 78-81.

[22]. Moore, D. S., & Kirkland, S. (2007). *The basic practice of statistics* (Vol. 2). New York: WH Freeman.

[23]. Boussaada, Z., Curea, O., Remaci, A., Camblong, H., & Mrabet Bellaaj, N. (2018). A nonlinear autoregressive exogenous (NARX) neural network model for the prediction of the daily direct solar radiation. *Energies*, *11*(3), 620.

[24]. Yassin, I. M., Taib, M. N., & Adnan, R. (2014). Extended analysis of bpso structure selection of nonlinear auto-regressive model with exogenous inputs (NARX) of direct current motor. *Songklanakarin Journal of Science & Technology*, *36*(6).

[25]. Hasnan, M. I., Jaffar, A., Thamrin, N. M., Misnan, M. F., Yassin, A. I. M., & Ali, M. S. A. M. (2021). NARX-based water quality index model of Air Busuk River using chemical parameter measurements. *Indonesian Journal of Electrical Engineering and Computer Science*, *23*(3), 1663-1673.

[26]. Thike, P. H., Zhao, Z., Liu, P., Bao, F., Jin, Y., & Shi, P. (2020). An early stopping-based artificial neural network model for atmospheric corrosion prediction of carbon steel. *CMC-Comput Mater Contin*, *65*(3), 2091-2109.

[27]. Barlas, Y. (1990). An autocorrelation function test for out put validation. *Simulation*, *55*(1), 7-16.

[28]. Barlas, Y. (1996). Formal aspects of model validity and validation in system dynamics. *System Dynamics Review: The Journal of the System Dynamics Society*, *12*(3), 183-210.

[29]. Dogan, G. (2007). Bootstrapping for confidence interval estimation and hypothesis testing for parameters of system dynamics models. *System Dynamics Review*, *23*(4), 415-436.

[30]. Du, Y. C., & Stephanus, A. (2018). Levenberg-Marquardt neural network algorithm for degree of arteriovenous fistula stenosis classification using a dual optical photoplethysmography sensor. *Sensors*, *18*(7), 2322.